RevMexAA (Serie de Conferencias), **10**, 101–108 (2001)

EXPLOSIONS DURING GALAXY FORMATION

Hugo Martel and Paul R. Shapiro

Dept. of Astronomy, University of Texas at Austin

RESUMEN

Consideramos una explosión en el centro de un halo que se forma por inestabilidad gravitacional en la intersección de filamentos en el plano de un 'pancake' cosmológico durante el colapso de éste como un modelo idealizado de los efectos de liberación de energía por supernovas durante la formación de las galaxias. Estos halos semejan los objetos virializados en las simulaciones de N–cuerpos en un universo MOF y, por lo tanto, sirven como modelo de prueba sin escala para formación de galaxias. Las simulaciones ASPH/P^{3}M revelan que tales explosiones son anisotrópicas. La energía y los metales se canalizan a las regiones de baja densidad, lejos del plano del 'pancake'. Este permanece esencialmente sin perturbaciones, aun cuando la explosión sea tan fuerte que aleje todo el gas que estaba dentro del halo en el inicio de la misma y recaliente el medio intergaláctico (MIG) que rodea al 'pancake'. La caída de materia rápidamente reemplaza este gas arrojado y gradualmente se restaura la fracción de gas a medida que la masa del halo continúa aumentando. Las estimaciones de la época del colapso y la liberación de energía por SNs para galaxias de masas diferentes en el modelo MOF pueden relacionar estos resultados a temas de separación y pérdida de masa dependientes de la escala y su implicación al calentamiento temprano del MIG y al enriquecimiento de metales así como a la creación de galaxias enanas dominadas por materia oscura.

ABSTRACT

As an idealized model of the effects of energy release by supernovae during galaxy formation, we consider an explosion at the center of a halo which forms at the intersection of filaments in the plane of a cosmological pancake by gravitational instability during pancake collapse. Such halos resemble the virialized objects found in N–body simulations in a CDM universe and, therefore, serve as a convenient, scale–free test–bed model for galaxy formation. ASPH/P^{3}M simulations reveal that such explosions are anisotropic. The energy and metals are channeled into the low density regions, away from the pancake plane. The pancake remains essentially undisturbed, even if the explosion is strong enough to blow away all the gas located inside the halo at the onset of the explosion and reheat the IGM surrounding the pancake. Infall quickly replenishes this ejected gas and gradually restores the gas fraction as the halo mass continues to grow. Estimates of the collapse epoch and SN energy–release for galaxies of different mass in the CDM model can relate these results to scale–dependent questions of blow–out and blow–away and their implication for early IGM heating and metal enrichment and the creation of dark–matter–dominated dwarf galaxies.

Key Words: **COSMOLOGY: THEORY — GALAXIES: FORMATION — HYDRODYNAMICS — INTERGALACTIC MEDIUM**

1. INTRODUCTION

The release of energy that occurs during galaxy formation can have important consequences for the structure and further evolution of these galaxies, other galaxies, and the intergalactic medium (IGM) in which they

form. Numerous observations cannot be explained by theoretical models unless energy release is invoked: e.g. (1) Observations reveal that dwarf spheroidal galaxies are dark–matter rich relative to normal galaxies (e.g. Gallagher & Wyse 1994). (2) Semi–analytical models of galaxy formation in a CDM universe (e.g. White & Frenk 1991) find that gas cooling is too efficient, leading to an overabundance of low–luminosity galaxies. (3) Simulations of galaxy formation fail to explain galactic rotation; too much gas angular momentum is transferred to the dark matter halo (e.g. Navarro & Steinmetz 1997). (4) N–body simulations of the CDM model predict an order of magnitude more dwarf satellite galaxies in the Local Group than are observed (e.g. Moore et al. 1999). (5) Observational limits on the H I Gunn–Peterson effect in the spectra of distant quasars indicate that the IGM at $z \gtrsim 5$ was already highly ionized (e.g. Songaila et al. 1999). (6) A heavy element abundance of 10^{-3} solar or more is ubiquitous in the Lyα forest at $z \gtrsim 3$, including that associated with gas at close to the mean IGM density (e.g. Ellison et al. 2000 and refs. therein). (7) Observations of intracluster gas in X–ray clusters indicate a heavy element abundance $\sim 1/3$ solar and excess entropy relative to the predictions of CDM simulations without energy–release (e.g. Loewenstein & Mushotzky 1996; Ponman, Cannon & Navarro 1999).

In this paper, we present 3D numerical gas dynamical simulations of the effect of energy release by supernovae, and the consequences of this energy release for the evolution of the halo in which the explosion takes place, the surrounding large–scale structure of which the halo is a part, and the IGM. Our first discussion of this work, based upon somewhat lower-resolution simulations, was in Martel & Shapiro (2000).

2. PANCAKE INSTABILITY AND FRAGMENTATION AS A TEST–BED FOR GALAXY FORMATION

Galaxy formation which leads to star formation results in supernova (SN) explosions and the resulting shock–heating and outward acceleration of interstellar and intergalactic gas. Previous attempts to model this effect have typically been along one of three lines, that which adopts a smooth initial gas distribution in a galaxy–like, fixed, dark–matter gravitational potential well (e.g. Mac Low & Ferrara 1999; Murakami & Babul 1999; Efstathiou 2000), that which considers a single, isolated, but evolving, density fluctuation (i.e. without merging, infall, or external tidal forces) (e.g. Katz 1992), and that in which the galaxy forms by condensation out of Gaussian–random–noise primordial density fluctuations such as in the CDM model (e.g. Cen & Ostriker 1992; Navarro & White 1993; Gnedin & Ostriker 1997; Katz, Weinberg & Hernquist 1997; Steinmetz 1997; Yepes et al. 1997). In the first two approaches, the computational ability to resolve shocks which propagate away from the sites of explosive energy release is generally higher, but because the galaxy is treated as isolated, the cosmological initial and boundary conditions leading to the formation of that galaxy are ignored. The third approach, which takes these initial and boundary conditions into account, is generally more realistic, but the resolving of shocks is generally quite poor.

Structure formation from Gaussian random noise proceeds in a highly anisotropic way, favoring the formation of pancakes and filaments over quasi–spherical objects. Our previous work (Valinia et al. 1997; Martel, Shapiro & Valinia 2001, in preparation; Alvarez, Shapiro & Martel 2001) has demonstrated, however, that a cosmological pancake, modeled as the nonlinear outcome of a single plane–wave density fluctuation, is subject to a linear gravitational instability which results in the formation of quasi–spherical lumps with density profiles similar to the universal halo profile found to fit the results of 3D N–body simulations in the CDM model (Navarro, Frenk & White 1997). This suggests that this 3D instability of cosmological pancakes may be used as an alternative to the details of the CDM model as a test–bed in which to study halo and galaxy formation further.

This approach provides a good compromise between the two limits discussed above. Since we are simulating a single galaxy, numerical resolution can be quite high, comparable to that of simulations which treat the galaxy as isolated. However, it provides a self–consistent cosmological origin and boundary condition for the galaxy, including the important effects of anisotropic gravitational collapse and continuous infall, while avoiding the complexity of simulations with Gaussian random noise.

3. SIMULATING THE EFFECT OF EXPLOSIVE ENERGY RELEASE ON GALAXY FORMATION

Our gas dynamical simulations are based upon the 3D ASPH algorithm (Shapiro et al. 1996; Owen et al. 1998; Martel & Shapiro 2001, in preparation), coupled to a P^3M gravity solver, with 64^3 particles each of gas and dark matter, and a P^3M grid of 128^3 cells with softening length $\eta = 0.3$ grid spacings. The initial

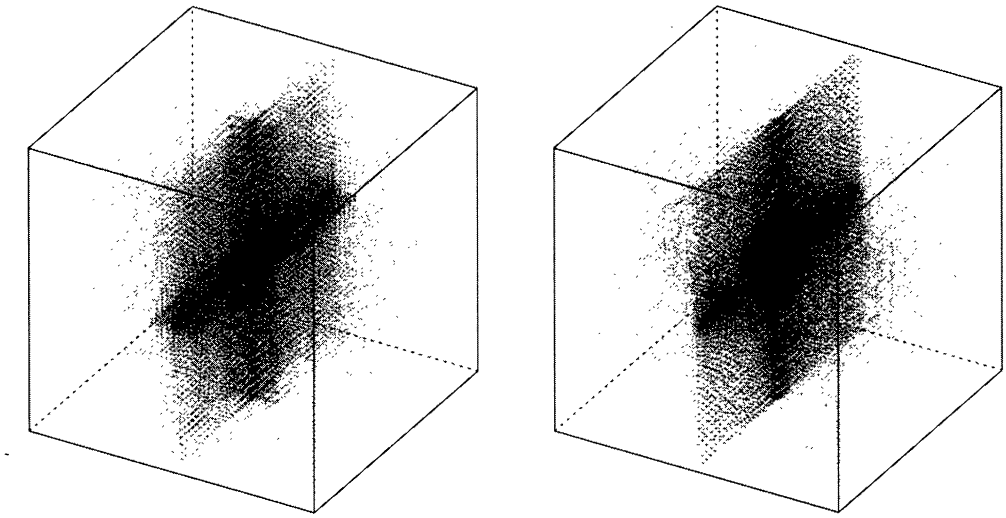

Fig. 1. (a) Dark matter particles at $a/a_c = 3.0$ for $\chi = 0$; (b) gas particles at $a/a_c = 3.0$ for $\chi = 100$.

conditions correspond to the growing mode of a single sinusoidal plane–wave density fluctuation, perturbed by two transverse perturbation modes of equal wavelength and amplitude equal to 1/5 of the amplitude of the primary pancake. We model the release of energy due to SNe in terms of a single impulsive explosion which may represent a starburst or the collective effect of multiple SNe. The explosion occurs when gas particles at the center of our dark matter halo first reach a density contrast relative to the average background density, $\rho_{\rm gas}/\langle\rho_{\rm gas}\rangle$, exceeding 10^3 (at $a_{\rm exp} = 1.912a_c$, where a_c is the scale factor at which the primary pancake mode leads to caustic formation in the dark matter and accretion shocks in the gas). We then deposit a certain amount of thermal energy $\chi\mathcal{E}_{\rm halo}$ in the center of the halo, distributed smoothly over the central particles and their nearest neighbors, where $\mathcal{E}_{\rm halo}$ is the total thermal energy of the gas whose density exceeds 200 times the cosmic mean gas density, and χ is a dimensionless constant. We have performed simulations for $\chi = 0$ (no explosion), $\chi = 10$ (modest explosion), $\chi = 100$ (strong explosion) and $\chi = 1000$ (blowaway regime). All simulations end at $a/a_c = 3$.

We consider an Einstein–de Sitter universe ($\Omega_0 = 1$) with baryon density parameter $\Omega_{\rm B} \ll 1$. In that case, the pancake problem is self–similar and scale–free (when radiative cooling and photoheating are ignored), as long as all lengths are expressed in units of the comoving pancake wavelength λ_p, time is expressed in terms of a/a_c, and the explosion energy is expressed in terms of the efficiency factor χ. This has the advantage that one simulation serves to model all possible masses and collapse epochs, for each value of χ. Our neglect of radiative cooling, a scale– and epoch–dependent process, amounts to the conservative limiting approximation with which to assess the minimum value of χ which leads to blow–away, metal–ejection, IGM shock–heating or the disturbance of the pancake. With cooling neglected, photoheating can also be safely neglected, except for the possibility that a photoheated background IGM (e.g. after reionization) might have a significant enough pressure to influence the outflow. We will evaluate the latter possibility in our discussion section. Without heating and cooling, the assumption $\Omega_{\rm B} \ll 1$ ensures that dark matter dominates the gravitational force everywhere and that our results are essentially independent of $\Omega_{\rm B}$. (Note: To be specific, we adopt $\Omega_{\rm B} = 0.03$.)

4. SCALE–FREE RESULTS

Figure 1(a) shows the pancake–filament–halo structure in the dark matter at $a/a_c = 3$, for the case without explosion. The dark matter is hardly affected by the gas, so Figure 1(a) represents, to very good accuracy, the final dark matter distribution for all cases, with and without explosions. Figure 1(b) shows the gas distribution for the intermediate case $\chi = 100$. The explosion expelled gas from the central halo into the low–

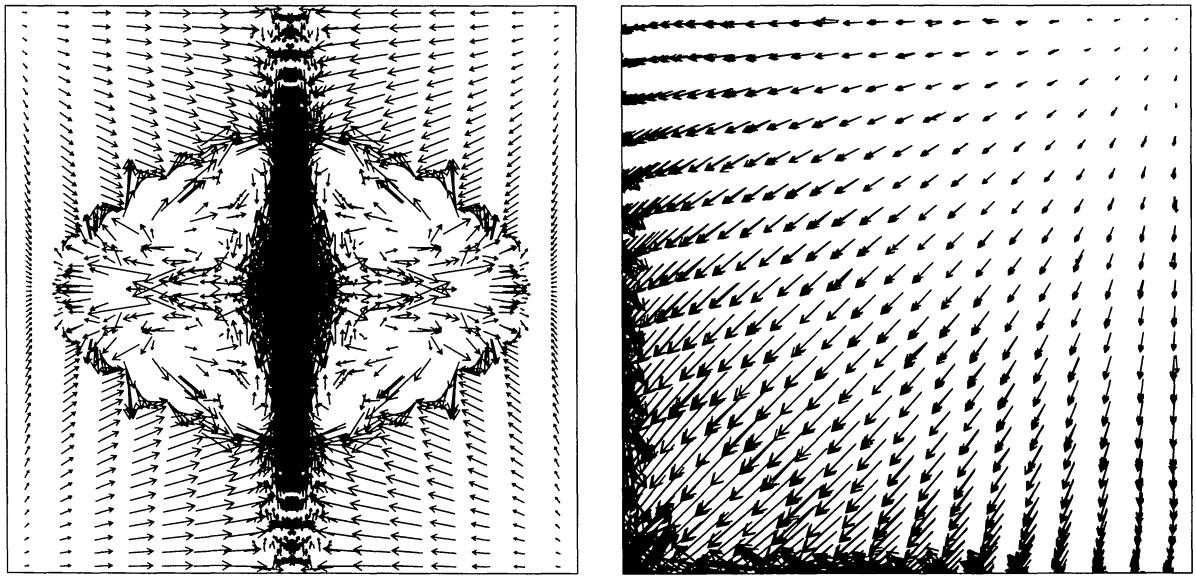

Fig. 2. Velocity field of gas at $a/a_c = 3.0$ for the case $\chi = 100$: (left) in the plane normal to the pancake, which bisects the halo, and (right) in the pancake plane.

density regions surrounding the pancake, sweeping out in the process exterior gas which was infalling along directions perpendicular to the pancake plane. For $\chi = 100$, the expelled gas fills an important fraction of the computational volume at $a/a_c = 3$, whereas for $\chi = 1000$, the expelled gas fills the entire volume outside the pancake–filament–halo structure. In all cases with explosion, we found that the pancake and filaments outside the halo are hardly affected.

Figure 2 shows the velocity field of the gas at $a/a_c = 3$ for the case $\chi = 100$ in the plane normal to the pancake (left panel) and in the pancake plane (right panel, only upper right quadrant plotted). The outer shock expanding into the low density regions is clearly visible on the left panel. The region bounded by this shock contains gas moving outward along the axis, forming a bipolar jet. The gas inside the pancake is still infalling toward the filaments and the central halo, hardly affected by the explosion. This infall will replenish the central halo with gas, although some of this replenishment is subsequently ejected in the bipolar jet. Neverthless, the halo eventually recovers most of its gas fraction.

The effect of the explosion in blowing gas away is illustrated by Figure 3. Both panels show a projection on the plane normal to the pancake at $a/a_c = 3$, with the edge–on pancake central plane and the halo represented by a vertical line and the large circle of radius r_{200}, respectively (where r_{200} is the radius within which the average total density is 200 times the cosmic mean). Gas particles which were located in the central halo (inside $r_{200} = 0.0229$) at the onset of explosion are shown in the left panel. The small open circles show the subset of 128 particles which were the original recipients of the explosion energy and, by implication, the metal–enriched SN ejecta. By $a/a_c = 3$, these particles have been ejected from the central halo, but none into the pancake. The right panel shows those gas particles which are located outside of the central halo at $a/a_c = 3$ that would have been inside in the absence of explosion. This is essentially the gas that was prevented from collapsing by the explosion. *Not a single particle that would have been located in the halo in the absence of the explosion ends up inside the surrounding pancake, away from the halo, instead.*

Without explosion, the total halo mass $M_{\rm tot}$, the dark matter mass $M_{\rm dm}$ and gas mass $M_{\rm gas}$ within r_{200} each grow by a factor of about 20 from the time of onset of the explosion to $a/a_c = 3$ (i.e. $a/a_{\rm exp} \cong 1.5$). For the dark matter, the halo mass $M_{\rm dm}$ grows by this same factor with or without explosion. This is an important difference between these simulations and those of Mac Low & Ferrara (1999), where explosions were triggered inside a relaxed object of fixed mass.

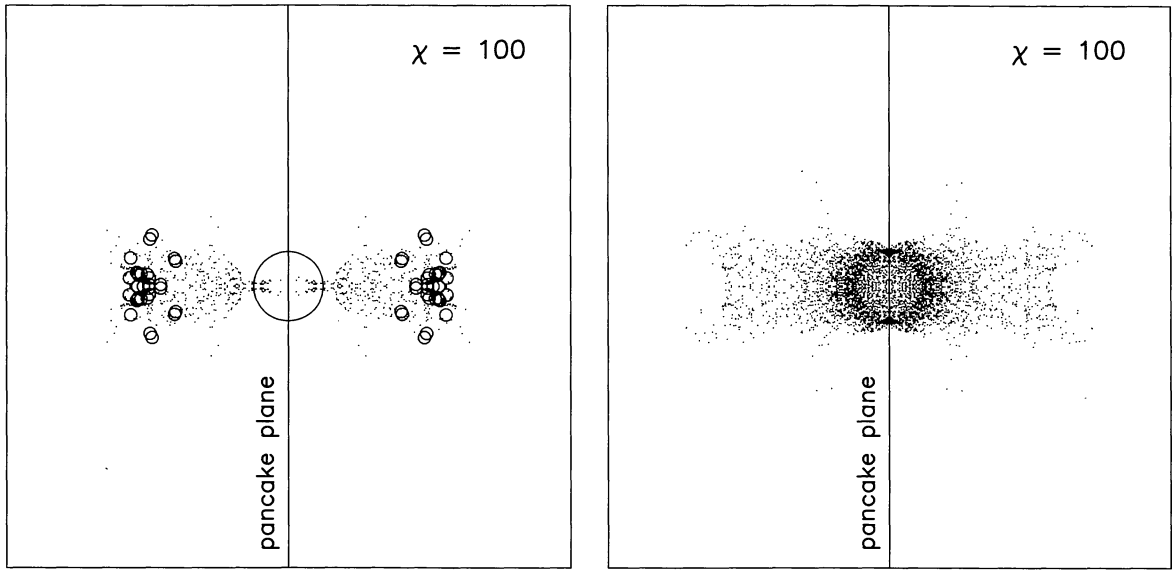

Fig. 3. (Left) Gas particles at $a/a_c = 3$ which were located inside the halo at onset of explosion (large circle radius = r_{200} at $a/a_c = 3$). Open circles show particles that have been enriched in metals. (Right) Gas particles located outside the halo at $a/a_c = 3.0$, that would have been inside if no explosion.

Our results indicate that the ability of explosions during galaxy formation to eject gaseous baryons and metals is dependent on the dimensionless energy–release efficiency χ. For a virialized halo at explosion onset, $\chi \gtrsim 1$ is in principle enough energy to "unbind" the gas inside the halo. However, this assumes that the halo gas shares the explosion energy equally; some may, instead, be ejected with more energy than it needs, thereby depriving other gas of the minimum it needs to escape. Even if the explosion energy is shared equally, however, gas which escapes from the halo may not escape from the gravitational pull of the surrounding pancake and filaments, and may, therefore, eventually fall back in. In a calculation like ours, with periodic, cosmological boundary conditions, it is not possible to identify a simple escape velocity against which to compare our outflows to determine what gas ultimately escapes, not only from its parent halo, but also from the surrounding pancake. Nevertheless, we can distinguish the following outcomes. For $\chi = 10$, relatively little of the initial halo gas is blown out of the halo. The ejected fraction includes the gas in which the explosion energy and metals were initially deposited, but ejection is only temporary, since it falls back in relatively quickly. For $\chi = 100$, almost 3/4 of the halo gas is blown out, including that which received the original explosion energy and metals. By $a/a_{\rm exp} \cong 1.5$, it appears that the metal–enriched gas is able to escape into the low–density valley between pancakes without falling back. Even so, infall along the pancake plane, especially along the filaments, replenishes the ejected halo gas so efficiently that by $a/a_{\rm exp} \cong 1.05$, the halo contains more gas than at the explosion onset, while by $a/a_{\rm exp} \cong 1.5$, it has an order of magnitude more gas than that, only 26% less than it would have had without explosion. Only for $\chi = 1000$ is the halo gas all blown away and the explosion products driven so far away so fast that they collide with their image gas expelled by the explosion which occurred simultaneously in the neighboring pancake, when the two explosion blast waves reach the same boundary from opposite sides. Amazingly enough, even this "blow–away" explosion fails to disturb the continuous equatorial rain of gas infalling from the surrounding pancake plane and filaments. By $a/a_{\rm exp} \cong 1.1$, the expelled gas is fully replenished, while by $a/a_{\rm exp} \cong 1.5$, the final halo gas mass is close to 45% of what it would have been with no explosion.

In short, $\chi \lesssim 10$ corresponds to the "fall–back" regime, unlikely to be able to eject metals to pollute the IGM or the surrounding pancake and filaments. Explosions with $\chi \sim 100$ are required for "blow–out" to occur, in which the gas which shared the original explosion energy and metals is ejected from the halo, but not all

the halo gas is ejected with it. A value of $\chi \sim 1000$ is required for "blow–away," in which all of the halo gas is expelled, the explosion shock–heats not only the halo gas, but all of the external IGM, as well, and the metals are thrown as far as the distance between neighboring galaxies.

5. APPLYING SCALE–FREE RESULTS TO SCALE–DEPENDENT GALAXY FORMATION

All the results presented in §4 are scale–free. In this section, we illustrate how we can apply these results to some particular scales of interest. We use our pancake–halo model as a generic description of structure formation at a particular length scale $\lambda = \lambda_p$. To relate this model to the more complex structures that form in the CDM model, we identify the redshift of pancake formation z_c with the redshift $z_{\rm NL}$ at which density fluctuations become nonlinear at the scale of λ_p. For an Einstein–de Sitter universe, our pancake–halo model corresponds to a "$\nu - \sigma$ density fluctuation" if $z_c = z_{\rm NL} = \nu\sigma_{\lambda_p} - 1$, where σ_{λ_p} is the linearly–extrapolated present rms density fluctuation at scale λ_p. We assume an untilted, cluster–normalized CDM model with $H_0 = 70\,{\rm km\,s^{-1}Mpc^{-1}}$ (i.e. $\sigma_8 = 0.53$). For each value of λ_p from 0.1 to 1 Mpc (comoving value, present units), we determine σ_{λ_p}, z_c, the explosion onset $z_{\rm exp}$, final redshift $z_f = (1 + z_c)/3 - 1$, the gas mass $M_{\rm gas}$ and total mass $M_{\rm tot}$ of the halo at $z_{\rm exp}$, the explosion energy $E_{\rm exp}$ (i.e. $\chi\mathcal{E}_{\rm halo}$), and the explosion efficiency $\epsilon \equiv E_{\rm exp}/M_{\rm gas}$. [Note: The comoving wavelength $\lambda_{\rm halo}$ which would encompass a mass equal to the halo mass at $a/a_c = a_{\rm exp}/a_c \cong 2$ in the unperturbed background universe is actually less than λ_p. Hence, in a CDM universe, fluctuations on the scale $\lambda_{\rm halo}$ on average grow to nonlinear amplitude *earlier* than those on the scale λ_p. This effect is partially compensated here by the fact that the actual nonlinear collapse epoch for a spherical fluctuation is later than that for a planar one of the same initial amplitude. Neverthless, our approach here tends to underestimate the redshift of halo formation and explosion relative to the predictions of, say, the Press–Schechter ("PS") approximation for halos of the same total mass. In the future, we will consider an alternative approach which more closely matches the epoch a_c of our pancake collapse model to the PS approximation. Our purpose here, however, is only to illustrate how one would go about relating our scale–free determination of the effects of a given explosion efficiency parameter χ to the real efficiencies expected for galaxies of different mass and collapse epochs. The net effect of a refinement of our prescription above for identifying the values of z_c to use for each λ_p in the CDM model will primarily be to make the results we describe below for $3 - \sigma$ fluctuations apply, instead, to "$\nu - \sigma$" fluctuations of lower ν.]

We have considered a wide range of values for the explosion parameter χ. However, for any particular scale λ_p, we can use Milky Way star formation efficiencies and IMF to estimate what a typical average value of χ, χ_λ, might be for that scale. The efficiency of energy ejection is $\epsilon = f_*\eta_{\rm SN}E_{\rm SN}$, where f_* is the star formation efficiency, defined as the fraction of halo gas that turns into stars, $\eta_{\rm SN}$ is the number of SNe expected per $M_\odot$ of stars formed, and $E_{\rm SN}$ is the amount of energy per SN available to drive the SN remnant blast wave after taking account of radiative losses in the ISM. We take $f_* = 0.05$ (Larson 1992; Lada, Strom & Myers 1993 and refs. therein), $\eta_{\rm SN} = 5 \times 10^{-3}M_\odot^{-1}$ (i.e. 1 SN per $200M_\odot$ of stars) (Murakami & Babul 1999; Efstathiou 2000; van den Bosch 2000), and $E_{\rm SN} = 10^{50}$ergs (Thornton et al. 1998). Equating this estimated "typical" ϵ with our simulation efficiencies $\epsilon = \chi\mathcal{E}_{\rm halo}/M_{\rm gas}$ for a given z_c and λ_p, we can then solve for χ_λ. Our results for $3 - \sigma$ fluctuations are listed in Table 1, including the implied number of SNe per explosion, both for any χ and also for $\chi = \chi_\lambda$. As we see, our chosen range of explosion intensities, $\chi = 10 - 1000$, covers all cases.

Our simulations show that $\chi \sim 100$ is required to eject metals into the IGM, while if $\chi \sim 1000$, the ejected gas and metals can travel all the way to the edge of the computational volume by $a/a_{\rm exp} \cong 1.5$. As Table 1 shows, for $3-\sigma$ fluctuations, a value of $\chi \sim 100$ corresponds to χ_λ only for $\lambda_p < 0.2\,{\rm Mpc}$ (halo $M_{\rm tot} < 10^7M_\odot$), while values as large as $\chi \sim 1000$ would require starburst efficiencies, well in excess of current Milky Way star–formation estimates. Our analysis also allows us to determine the metallicity yield implied by those explosions in such halos and the implied space–averaged heavy element abundance of the IGM. We will discuss that in a future paper. We note that our qualitatively new result here, that even the most violent explosions which blow gas away and eject metals nevertheless permit the parent halo to replenish its lost gas in a fraction of a Hubble time, may enable a single halo to contribute multiple outbursts.

In the current scale–free simulations, the IGM in the background universe is assumed to be cold enough that the actual pressure of the IGM is negligible compared to that of the gas heated either by the pancake accretion shocks or the explosion–generated shocks. The evolution of the shocked pancake gas and the explosion, in that case, are unaffected by the pressure of the IGM. As long as the pancake collapse and the explosion took

TABLE 1

ILLUSTRATIVE VALUES FOR $3-\sigma$ FLUCTUATIONS IN THE SCDM MODEL

λ_p(Mpc)	z_c	$z_{\rm exp}$	z_f	$M_{\rm tot}(M_\odot)$	$M_{\rm gas}(M_\odot)$	$N_{\rm SN}$	χ_λ	$N_{\rm SN}(\chi=\chi_\lambda)$
1.00	8.81	4.13	2.27	1.37×10^9	3.36×10^7	$2.95\times10^3\chi$	2.84	8380
0.30	15.80	7.79	4.60	3.71×10^7	9.08×10^5	$1.23\times10^1\chi$	18.52	227
0.20	18.56	9.23	5.52	1.10×10^7	2.70×10^5	$1.88\times10^0\chi$	35.92	68
0.10	23.66	11.90	7.22	1.37×10^6	3.36×10^4	$7.41\times10^{-2}\chi$	113.38	8

place before reionization of the IGM, this is a correct description independent of the actual mass–scale of the pancake. If reionization took place before the explosion, however, that would have raised the pressure of the background IGM relative to that in our current simulations. Ferrara, Pettini & Shchekinov (2000) and Murakami & Babul (1999) suggest that the ejection of gas and metals to large distances from early galaxies would have been inhibited by the pressure of the IGM. One concern, then, is that the efficiency of metal ejection found in our simulations might be an artifact resulting from underestimating the IGM pressure. To check this, we compared the total pressure $P_{\rm metals}$ of the ejecta (ram pressure + thermal pressure) to what the actual value of the IGM pressure, $P_{\rm IGM}$, would have been if the IGM temperature following reionization were 10^4K, for halos of different mass forming at different epochs. For $1-\sigma$ fluctuations, for $\chi=100$, $P_{\rm metals}/P_{\rm IGM}>1$ for $\lambda_{\rm p}\geq 0.60\,$Mpc, while for $\chi=1000$, $P_{\rm metals}/P_{\rm IGM}>1$ for $\lambda_{\rm p}\geq 0.20\,$Mpc. For $3-\sigma$ fluctuations, instead, for $\chi=100$, $P_{\rm metals}/P_{\rm IGM}>1$ for $\lambda_{\rm p}\geq 0.30\,$Mpc, while for $\chi=1000$, $P_{\rm metals}/P_{\rm IGM}>1$ for $\lambda_{\rm p}\geq 0.10\,$Mpc. Our results are therefore valid even if reionization occurred before the explosion, except at small mass scales, where the IGM pressure might very well prevent the ejection of metals over large distances.

All of the halos in Table 1 appear to form and evolve early enough to cause widespread heavy element distribution prior to $z=3$, as required to explain the ubiquitous metallicity of the IGM measured in Lyman–α forest absorption spectra. The smaller mass objects are the ones for which the smaller binding energy per gram is more easily overcome by any given star formation and supernova efficiency, if the latter are assumed to be independent of mass across the mass spectrum of halos. Only the smallest mass objects in Table 1, in fact, can expect to do so if they are limited to efficiencies typical for the Milky Way. Such small mass halos are precisely the ones which are able to form early enough that they may, indeed, do their exploding *before* the reionization and reheating of the IGM is complete. If not, then efficiencies much larger than those of the current Milky Way are probably required, if explosions from those objects are to succeed in blowing the heavy elements into the IGM in the face of the opposing boundary pressure of the IGM once the latter has been reionized.

A final determination of the success or failure of heavy element distribution by SN explosions following star formation in low–mass halos which form at high redshift, we conclude, will depend sensitively on the efficiencies of star formation and supernova energy release, as well as the relative timing of these explosions versus universal reionization, details which are highly uncertain at this time. Our results support the conjecture that heavy element distribution at the observed level of $\approx 10^{-3}$ solar in the IGM was accomplished prior to the completion of reheating which accompanied universal reionization, by a smaller fraction of the condensed baryons in the universe than later were responsible for completing the reionization by starlight or quasars.

6. SUMMARY AND CONCLUSION

We have simulated explosions inside cosmological halos which form by gravitational instability during the collapse of a cosmological pancake. This is a test–bed model that can be used to describe explosions during galaxy formation under more realistic circumstances, such as that involving Gaussian random noise initial conditions. Our results include the following: (1) Blow–out and blow–away are generically anisotropic events which channel energy, mass loss, and metal–enrichment outward preferentially along the symmetry axis of the local pancake and away from the intersections of filaments in the pancake plane. This anisotropy has a very different origin from that of the blow–outs in Mac Low & Ferrara (1999), which occurred in a rotationally–flattened gaseous disk inside an isolated, spherical halo of dark matter, where the rotational–flattening introduced an axisymmetry into the problem. (2) Shock waves propagate into the IGM on both sides of the pancake, heating

the gas up to temperatures comparable to or greater than the characteristic virial temperature of the halo which initiated the explosion. (3) Even with explosions which are strong enough to propagate the shock waves all the way to the boundary of the computational volume, thereby filling the universe with overlapping explosions which reheat the entire IGM, the condensed structure in which the explosion takes place is hardly disturbed. (4) The explosion does not halt the continuous infall of gas from the surrounding pancake and filaments into the halo. This infall replenishes the halo gas and gradually restores its gas fraction. As a result, the same halo may be able to experience multiple explosions.

We are pleased to acknowledge stimulating discussions with Richard Mushotzky. This work was supported by NASA Grants NAG5–7363 and NAG5–7821, NSF Grants ASC–9504046, Grant 3658–0624–1999 from the Texas Advanced Research Program, and the High Performance Computing Facility, University of Texas.

REFERENCES

Alvarez, M., Shapiro, P. R. & Martel, H. 2001, in "The Seventh Texas–Mexico Conference on Astrophysics: Flows, Blows, and Glows," eds. W. Lee and S. Torres–Peimbert, RevMexAA (Serie de Conferencias) (these proceedings)
Cen, R. & Ostriker, J. P. 1992, ApJ, 399, L113
Efstathiou, G. 2000, MNRAS, 317 ,697
Ellison, S. L., Songaila, A., Schaye, J. & Pettini, M. 2000, AJ, 120, 1175
Ferrara, A., Pettini, M. & Shchekinov, Y. 2000, MNRAS, 319, 539
Gallagher, J. S. & Wyse, R. F. G. 1994, PASP, 106, 706
Gnedin, N. Y. & Ostriker, J. P. 1997, ApJ, 486, 581
Katz, N. 1992, ApJ, 391, 502
Katz, N., Weinberg, D. H. & Hernquist, L. 1997, ApJS, 105, 19
Lada, E. A., Strom, K. M. & Myers, P. C. 1993, in Protostars and Planets III, eds. E. Levy & J. I. Lunine (University of Arizona Press), p. 245
Larson, R. B. 1992, in Star Formation in Stellar Systems (III Canary Islands Winter School of Astrophysics), eds. G. Tenorio–Tagle, M. Prieto & F. Sánchez (Cambridge University Press), p. 127.
Loewenstein, M. & Mushotzky, R. F. 1996, ApJ, 466, 695
Mac Low, M.-M. & Ferrara, A. 1999, ApJ, 513, 142
Martel, H. & Shapiro, P. R. 2000, Nucl. Phys. B, 80, 09/11 (astro–ph/9904121)
Moore, B., Ghigna, S., Governato, F., Lake, G., Quinn, T., Stadel, J., & Tozzi, P. 1999, ApJ, 524, L19
Murakami, I. & Babul, A. 1999, MNRAS, 309, 161
Navarro, J. F., Frenk, C. S. & White, S. D. M. 1997, ApJ, 490, 493
Navarro, J. F. & Steinmetz, M. 1997, ApJ, 478, 13
Navarro, J. F. & White, S. D. M. 1993, MNRAS, 265, 271
Owen, J. M., Villumsen, J. V., Shapiro, P. R. & Martel, H. 1998, ApJS, 116, 155
Ponman, T. J., Cannon, D. B. & Navarro, J. F. 1999, Nature, 397, 135
Shapiro, P. R., Martel, H., Villumsen, J. V. & Owen, J. M. 1996, ApJS, 103, 239
Songaila, A., Hu, E. M., Cowie, L. L. & McMahon, R. G. 1999, ApJ, 525, L5
Steinmetz, M. 1997, in Structure and Evolution of the Intergalactic Medium from QSO Absorption Line Systems, eds. P. Petitjean and S. Charlot (Paris: Editions Frontières), p. 281
Thornton, K., Gaudlitz, M., Janka, H.-Th. & Steinmetz, M. 1998, ApJ, 500, 95
Valinia, A., Shapiro, P. R., Martel, H. & Vishniac, E. T. 1997, ApJ, 479, 46
van den Bosch, F. C. 2000, ApJ, 530, 177
White, S. D. M. & Frenk, C. S. 1991, ApJ, 379, 52
Yepes, G., Kates, R., Khokhlov, A. & Klypin, A. 1997, MNRAS, 284, 235

Hugo Martel and Paul R. Shapiro: Department of Astronomy, University of Texas, Austin, TX 78712, USA (hugo@simplicio.as.utexas.edu, shapiro@astro.as.utexas.edu).